ROLLER NIP DEFLECTIONS

By

Kevin Cole & Brooks Schneider
Optimation Technology, Inc.
USA

ABSTRACT

Rubber covered nip rollers are used in many web handling and processing applications. Successful use of these systems requires an accurate knowledge of the impact of various design and process parameters on key response metrics such as nip pressure and surface speed axial uniformity. These metrics are important since they are directly correlated to operational and functional requirements of nipping processes. Axial variations occur primarily due to roller shell bending, which arise from externally applied end loading forces. The non-linear radial compressive characteristics of elastomeric coverings that are often a part of such systems contributes to system complexity. Previous papers have presented a two-dimensional analytical model that relates force and deformations of rubber rollers in contact with other rollers. In the present paper, a three-dimensional model is presented that extends the previous model by incorporating shell bending deflections. In addition to the non-linearity due to the compressive characteristics of rubber coverings, the model also includes the ability to include other non-linear effects such as roller diameter non-uniformity and misalignment, or skew, of the roller's rotation axes. The model is used to demonstrate that the use of crowning or skewing must not only account for geometric effects but also for the nearly incompressible nature of rubber coverings to successfully mitigate axial nip pressure variation that otherwise is present in end-loaded nip roller systems.

NOMENCLATURE

B	journal length, m
E	shell material elastic modulus, Pa
F	journal loading, N
I	shell flexural stiffness, m^4
k	stiffness of the elastic foundation, N/m^2
r	roller radius, m
w	shell half width, m

δ   nip roller pair shell centerline relative radial deflection (and rubber engagement when gapping is not present), m

Subscripts

1, 2   lower, upper rollers in nip roller system (see Figure 1)

INTRODUCTION

Rubber covered nip rollers are used in many web handling and web processing applications. In typical situations, a rubber covered nip roller will be used in combination with a hard-surfaced metal backing roller to develop contact across the width (e.g., "*nip width*") and along the machine direction (e.g., "*nip footprint*"). Examples of nip roller systems where this configuration is typical include nip roller tension drives where the rubber covered nip roller is added to increase traction and lamination nip drives where the rubber covered nip roller provides the capability to spatially manage contact area and pressure, which is required to achieve successful lamination between two or more webs. Nip roller systems are generally fixed force or displacement loaded through journals extending beyond the ends of roller shells. Figure 1 shows such a configuration where the upper roller is hard surfaced and the lower surface consists of a rubber (e.g., elastomer) covering.
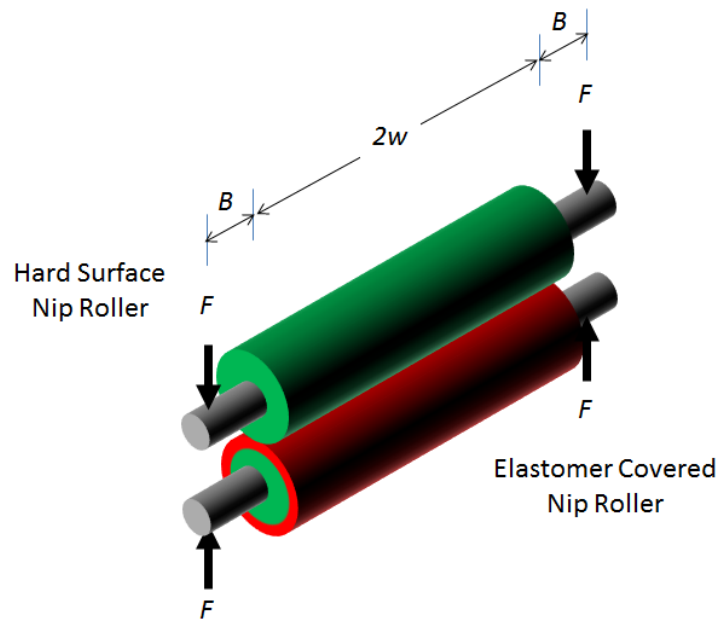

Figure 1 – Typical Nip Roller System

Owing to the flexibility of roller shells, nip roller systems will tend to develop axially-nonuniform roller shell centerline relative radial deflections. This behavior will result in axially variable footprint lengths with the typical result that the footprint is larger at the ends and smaller midway across the width. The magnitude of this nonuniformity

will be a function of the relative bending stiffness's of the roller shells and the compressive stiffness of the rubber covering. This behavior is commonly understood and several authors have not only described the process implications (Roisum [1]) but have also provided analyses of varying degrees of complexity to model the axial nonuniformities that arise (Cole [2] and Good [3]).

Depending on the application, suggestions have been made as to how to compensate for the shell-deflection induced nonuniformities. Two examples include introducing a relative skew between the two roller rotation axes or adding diameter non-uniformity (e.g., *crowning*) to either one or the other of the two rollers. Such options are not necessarily the best option but in certain situations where pressure and footprint uniformity is of primary concern (such as laminating) and conditions do not allow for sufficient stiffening of the roller shells by other means, these options may be appropriate.

The purpose of this paper is to develop a 3-D nip model that has the capability to analyze the relative contributions of shell deflection, roller skew and diameter nonuniformity on rubber compression (e.g., *engagement*) and footprint axial nonuniformity. First, the model for performing this analysis is presented. The analysis is then used to quantitatively analyze how much skew and diameter non-uniformity is required to compensate for shell deflection. The analysis combines the results from the 2-D model developed by Cole [2] into a nonlinear 3-D model that builds on the-beam-on-an-elastic-foundation approach verified to be accurate for these applications by Good [3]. The model presented here; however, is more general in that it not only accommodates nonlinearity associated with compression in the rubber cover (where centerline relative radial deflection equals rubber engagement) but that also accommodates geometric nonlinearity associated with skew and diameter variations (where centerline relative radial deflection need not equal rubber engagement). The model assumes symmetry about the axial centerline of the nip roller pair but is otherwise quite general. For purposes of this paper, this limitation is insignificant; however, if can be easily relaxed by modification of the boundary conditions.

THE MODEL

The model that follows is presented in four stages. First, the differential equation, boundary conditions and solution is presented for a nip system consisting of a beam (roller shell deflection) on an elastic foundation (rubber covering) where the stiffness of the elastic foundation is assumed to be constant. Next, this solution is extended to incorporate the non-linear nature of the 2-D compressive behavior of the rubber covered nip roller system. This is achieved by using a transfer matrix approach that utilizes the linear solution to capture the impact of the non-linear radial stiffness dependency on rubber engagement. At this point, shell centerline relative radial deflection and rubber engagement are equal and the model is equivalent to that presented by Good [3]. The third stage presents modifications to the model to enable the inclusion of roller axes skew and roller crowning, which is described in the fourth stage. Key to enabling these capabilities is the addition, in the third stage, of the ability to handle arbitrary radial gapping; e.g., variable radial offset along the roller axis either prior to, or during, loading. By means that will be shown, this relaxes the constraint imposed by previous models that the shell centerline relative radial deflection and the rubber engagement be equal.

<u>**The Linear Model**</u>

The linear model treats the radial stiffness of the rubber covering as a Winkler foundation and the deflection of the roller shells as Euler beams. Figure 2 shows the

system geometry along with definitions for positive moment, shear and distributed load. The differential equation for the nip roller pair shell centerline relative radial deflection is given by:

$$\frac{d^4\delta}{dz^4} + \frac{k}{EI}\delta = 0 \qquad \{1\}$$

where the EI is the flexural stiffness of the combined system:

$$EI = \left(\frac{1}{(EI)_1} + \frac{1}{(EI)_2}\right)^{-1} \qquad \{2\}$$

The subscripts represent the lower and upper rollers shown in Figure 1 respectively. The boundary conditions are given by:

$$at\ z = 0, moment = -FB \longrightarrow \frac{d^2\delta}{dz^2}(z = 0) = \frac{FB}{EI}$$

$$at\ z = 0, shear = F \longrightarrow \frac{d^3\delta}{dz^3}(z = 0) = \frac{F}{EI}$$

$$at\ z = w, slope = 0 \longrightarrow \frac{d\delta}{dz}(z = w) = 0$$

$$at\ z = w, shear\ force = 0 \longrightarrow \frac{d^3\delta}{dz^3}(z = w) = 0 \qquad \{3\}$$
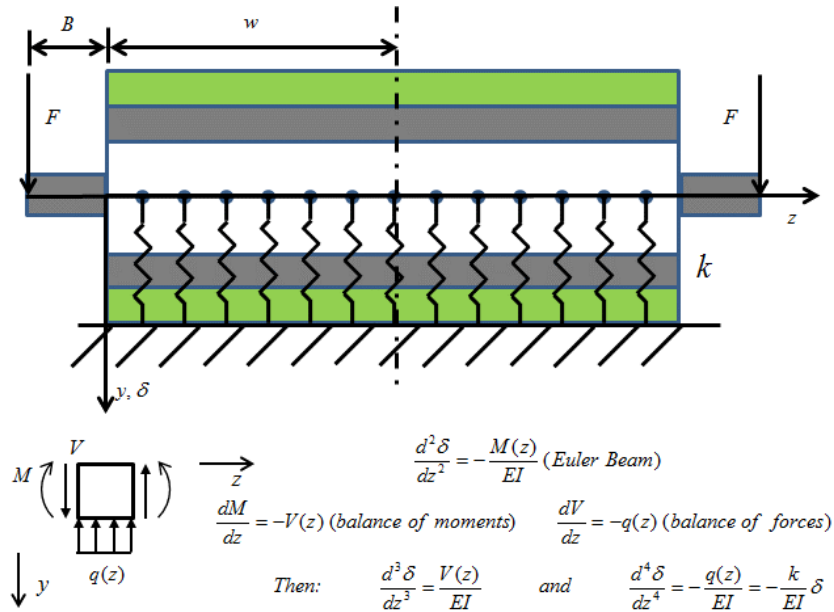

Figure 2 – Linear Model of a Rubber Covered Roller System

The foundation stiffness, k, is assumed to be constant for the linear model. The solution to the differential equation takes the following form:

$$\delta(z) = e^{\eta z}\{g_1 \cos \eta z + g_2 \sin \eta z\} + e^{-\eta z}\{g_3 \cos \eta z + g_4 \sin \eta z\} \qquad \{4\}$$

where $\eta = \sqrt[4]{\dfrac{k}{4EI}}$ is a parameter that represents the relative contribution of the rubber stiffness versus the flexural rigidity of the shells and the coefficients are constants of integration. Application of the boundary conditions yields the following matrix expression for the integration constants (where $c \equiv \cos \eta w$ and $s \equiv \sin \eta w$):

$$\begin{bmatrix} 0 & 2\eta^2 & 0 & -2\eta^2 \\ -2\eta^3 & 2\eta^3 & 2\eta^3 & 2\eta^3 \\ \eta e^{\eta w}(c-s) & \eta e^{\eta w}(c+s) & -\eta e^{-\eta w}(c+s) & \eta e^{-\eta w}(c-s) \\ -2\eta^3 e^{\eta w}(c+s) & 2\eta^3 e^{\eta w}(c-s) & 2\eta^3 e^{-\eta w}(c-s) & 2\eta^3 e^{-\eta w}(c+s) \end{bmatrix} \begin{Bmatrix} g_1 \\ g_2 \\ g_3 \\ g_4 \end{Bmatrix} = \begin{Bmatrix} \frac{FB}{EI} \\ \frac{F}{EI} \\ 0 \\ 0 \end{Bmatrix} \qquad \{5\}$$

Equation {5} can be inverted to give the integration constants from which the final solution can be written by substitution into {4}.

The Nonlinear Model

In this section, the linear model developed above is extended to account for the nonlinear 2-D load/engagement behavior of a typical force loaded nip system. In reference [2], a theoretical model was developed to predict nip footprint, nip load and creep[1] as a function of nip engagement. The method was developed by first formulating the exact solution to a linear elastic strip and then using equations of kinematic and force constraint to apply the solution to nip systems. Formulation of the plane strain model in terms of dilatational and deviatoric stress components enabled the elastomeric covering material to be modeled as incompressible.

The results from this model indicate that the load versus engagement relationship is nonlinear and then, since foundation stiffness is equal to the derivative of the load function, that the foundation stiffness is nonlinear as well. We proceed with the analysis of this section by assuming the load/engagement relationship can be approximated by the following relationship, as shown in Figure 3:

$$q(z) = \begin{cases} r\delta^s, & \delta > 0 \\ 0, & \delta \leq 0 \end{cases} \qquad \{6\}$$

During this stage, the shell centerline relative radial deflection is always positive and hence, we can use the terminology of shell deflection and rubber engagement interchangeably. Taking the derivative of {6}, we then find for the foundation stiffness the following nonlinear expression:

$$k(\delta) = \frac{dq}{d\delta} = rs\delta^{s-1} \qquad \{7\}$$

The constants *r* and *s* are found from a least-squares curve fit of the load/engagement relationship for the nip system of interest using the model from reference [2].

---

[1] Creep is defined as the tendency of rubber nips to convey webs at speeds that are slightly different than surface speed of the roller outside of the nip [2]

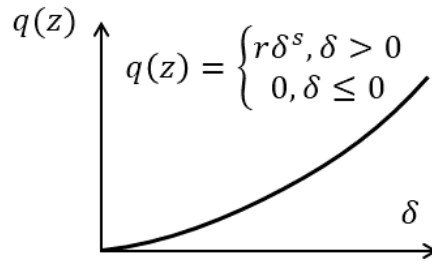$$q(z) = \begin{cases} r\delta^s, \delta > 0 \\ 0, \delta \leq 0 \end{cases}$$

Figure 3 – Load/Engagement Functional Relationship [2]

To proceed, we divide half of the beam into N sections and N+1 stations as indicated in Figure 4. We then apply the differential equation {1} to each section for a differential portion of the total load. The foundation stiffness of each section is determined from {7} and will be a function of engagement at the midpoint of each section, where the engagement will now be a function of position and load increment.

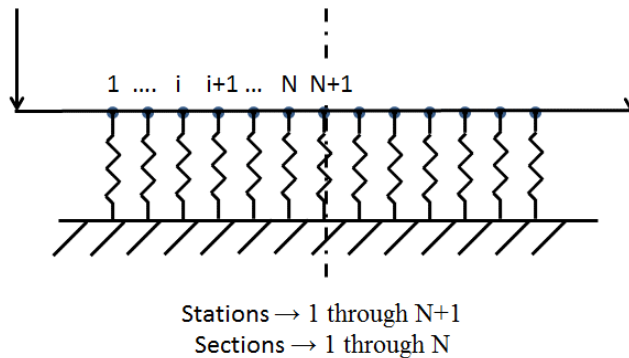Stations → 1 through N+1
Sections → 1 through N

Figure 4: Nip Roller System Discretization Scheme

For each load increment, we utilize the linear solution to determine the resulting incremental engagement at each station as follows. First, we develop a transfer matrix that relates incremental engagement, slope, moment and shear between stations. Next, we combine the individual transfer matrices into a single transfer matrix that relates the incremental engagement, slope, moment and shear between the first and last stations. Then, we impose incremental boundary conditions of the form expressed in {3}. By matrix inversion, we can then determine the unknowns at station 1 (e.g., the incremental engagement and the incremental slope) and from there, determine the incremental engagement at the remaining stations by using the transfer matrices. The axial distribution of engagement is then updated to give the cumulative engagement after each increment of loading. The final distribution of engagement is determined by repeating the process for all loading increments.

The key to this technique is the development of the transfer matrix across sections and then, assembly of the individual matrices into a global transfer matrix that allows for the application of the boundary conditions. We now describe this process. First, for an arbitrary section, say the ith, we must evaluate the constants of the solution to the

differential equation. In matrix form, we can write the differential engagement, slope, moment and shear at station i in terms of the solution constants as follows (and noting that we have aligned the local origin to station i):

$$
\begin{Bmatrix} \delta \\ \frac{d\delta}{dz} \\ \frac{d^2\delta}{dz^2} \\ \frac{d^3\delta}{dz^3} \end{Bmatrix}^i = \begin{bmatrix} 1 & 0 & 1 & 0 \\ \eta_i & \eta_i & -\eta_i & \eta_i \\ 0 & 2\eta_i^2 & 0 & -2\eta_i^2 \\ -2\eta_i^3 & 2\eta_i^3 & 2\eta_i^3 & 2\eta_i^3 \end{bmatrix} \begin{Bmatrix} g_1 \\ g_2 \\ g_3 \\ g_4 \end{Bmatrix}_i \qquad \{8\}
$$

In this expression, the superscripts indicate station location and the subscripts indicate evaluation at the midpoint of the section. It is also to be understood, while not explicitly indicated, that the responses and coefficients are incremental corresponding to the load increment. This expression is determined by evaluating {4} and its derivatives at the local origin and by computing η_i at the midpoint of the section based on the cumulative engagement up to this loading increment.

Equation {8} can be written symbolically as (where Δ and g are vectors representing the left-hand side and the solution coefficients of {8} respectively):

$$
\{\Delta\}^i = [A]_i\{g\}_i \qquad \{9\}
$$

The coefficient vector can now be found by matrix inversion:

$$
\{g\}_i = [A]_i^{-1}\{\Delta\}^i \qquad \{10\}
$$

At the i+1 station, we can similarly write the following:

$$
\begin{Bmatrix} \delta \\ \frac{d\delta}{dz} \\ \frac{d^2\delta}{dz^2} \\ \frac{d^3\delta}{dz^3} \end{Bmatrix}^{i+1} =
$$

$$
\begin{bmatrix} e^{\eta_i z_s}c_i & e^{\eta_i z_s}s_i & e^{-\eta_i z_s}c_i & e^{-\eta_i z_s}s_i \\ \eta_i e^{\eta_i z_s}(c_i - s_i) & \eta_i e^{\eta_i z_s}(c_i + s_i) & -\eta_i e^{-\eta_i z_s}(c_i + s_i) & -\eta_i e^{-\eta_i z_s}(s_i - c_i) \\ \eta_i^2 e^{\eta_i z_s}(-2s_i) & \eta_i^2 e^{\eta_i z_s}(2c_i) & \eta_i^2 e^{-\eta_i z_s}(2s_i) & \eta_i^2 e^{-\eta_i z_s}(-2c_i) \\ 2\eta_i^3 e^{\eta_i z_s}(-c_i - s_i) & 2\eta_i^3 e^{\eta_i z_s}(c_i - s_i) & 2\eta_i^3 e^{-\eta_i z_s}(c_i - s_i) & 2\eta_i^3 e^{-\eta_i z_s}(c_i + s_i) \end{bmatrix} \begin{Bmatrix} g_1 \\ g_2 \\ g_3 \\ g_4 \end{Bmatrix}_i \qquad \{11\}
$$

where z_s is the section width, $c_i = cos\eta_i z_s$ and $s_i = sin\eta_i z_s$. Symbolically, {11} can be written as:

$$
\{\Delta\}^{i+1} = [B]_i\{g\}_i \qquad \{12\}
$$

which becomes the following when combined with {10}:

$$
\{\Delta\}^{i+1} = [B]_i[A]_i^{-1}\{\Delta\}^i \equiv [G]_i\{\Delta\}^i \qquad \{13\}
$$

Expression {13} can be repeated for each section. Ultimately, we are then able to generate an expression relating the engagement and its derivatives at station N+1 to that at station 1:

$$\{\Delta\}^{N+1} = [B]_N[A]_N^{-1} \dots [B]_1[A]_1^{-1}\{\Delta\}^1 = [G]_N \dots [G]_1\{\Delta\}^1 \equiv [G]\{\Delta\}^1 \qquad \{14\}$$

We can now apply the boundary conditions to {14} to solve for the unknown incremental engagement and slope at station 1. The boundary conditions are like those in {3} but with the exception that here the values are those in {3} divided by the number of loading steps, n:

$$\begin{Bmatrix} \delta \\ 0 \\ \frac{d^2\delta}{dz^2} \\ 0 \end{Bmatrix}^{N+1} = [G] \begin{Bmatrix} \delta \\ \frac{d\delta}{dz} \\ \frac{FB}{nEI} \\ \frac{F}{nEI} \end{Bmatrix}^1 \qquad \{15\}$$

Expression {8} can readily be solved for the unknowns since there are 4 equations and 4 unknowns (incremental engagement and moment at station N+1 and incremental engagement and slope at station 1). Once the incremental engagement and slope is known at station 1, the transfer matrices can be used to determine incremental engagement across the entire nip roller. The final solution is obtained by repeating this process for all loading increments.

Addition of Gapping
To study the effect of roller axes skewing and roller diameter crowning, the model must be upgraded to enable the implementation of diameter non-uniformity. Key to developing this capability is the need to enable the model to handle the situation where the rubber engagement within a section is equal to zero (e.g., the nip roller shell centerline relative radial deflection is no longer equal to the rubber cover engagement). Such a situation will obviously be present when rollers are either skewed or crowned as loading increases from zero to the final load. However, even when rollers are aligned and cylindrical, there is the possibility that this situation might develop in end loaded nip roller systems. For example, nip roller systems with relatively low flexural stiffness shells, high rubber cover stiffness and long journals are prone to lift off between the two rollers mid-way across the shell. To accommodate this behavior in the non-linear model, the transfer matrix must be modified to handle sections where the cumulative engagement is equal to zero. When this is the case, the governing differential equation for the shell centerline relative radial deflection simplifies to the following since distributed external loading is not present (e.g., there is no compression in the rubber):

$$\frac{d^4\delta_{in}^i}{dz^4} = 0 \qquad \{16\}$$

The solution to {16} in terms of integration constants is as follows:

$$\delta_{in}^i = g_1 z^3 + g_2 z^2 + g_3 z + g_4$$

$$\frac{d\delta_{in}^i}{dz} = 3g_1 z^2 + 2g_2 z + g_3$$

$$\frac{d^2\delta_{in}^i}{dz^2} = 6g_1 z + 2g_2$$

$$\frac{d^3\delta_{in}^i}{dz^3} = 6g_1 \qquad \{17\}$$

The transfer matrix for a section where cumulative engagement has not yet occurred can be developed following the same approach as was used to develop {13}. For this case the two matrices are as follows:

$$[A]_i = \begin{bmatrix} 0 & 0 & 0 & 1 \\ 0 & 0 & 1 & 0 \\ 0 & 2 & 0 & 0 \\ 6 & 0 & 0 & 0 \end{bmatrix}, \quad [B]_i = \begin{bmatrix} z_s^3 & z_s^2 & z_s & 1 \\ 3z_s^2 & 2z_s & 1 & 0 \\ 6z_s & 2 & 0 & 0 \\ 6 & 0 & 0 & 0 \end{bmatrix} \qquad \{18\}$$

where again the incremental loading dependency of the coefficients and responses are not explicitly indicated. From these, the transfer matrix across the non-contacting section, $[G]_i$, can be generated per {13}. The non-linear model now uses the appropriate form of the transfer matrix during the solution process depending on whether the cumulative engagement is positive or zero.

One additional modification is required to enable the model to have the capability to handle symmetrical, but arbitrary initial diameter non-uniformity. Figure 5 shows how the load/engagement functional relationship, for diameter non-uniformity, is characterized by an axially dependent function (where δ_0 is the axially dependent variation in radius of the roller pair):

$$q(z) = \begin{cases} r(\delta - \delta_0)^s, & \delta > \delta_0 \\ 0, & \delta \leq \delta_0 \end{cases} \qquad \{19\}$$

The foundation stiffness, as before, is the derivative of {19}. By adding this capability into the non-linear model, we are now able to specify initial radius as an arbitrary function of axial location as indicated in Figure 6. The model, which can now handle gapping, now allows for a general specification of roller diameter along the axis. It should be noted that it is not important as to how the specified diameter variation is distributed between the lower and upper rollers since what is important is the relative difference between the two.
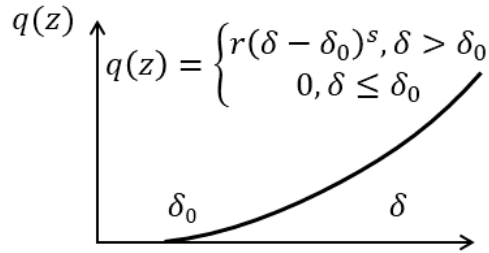

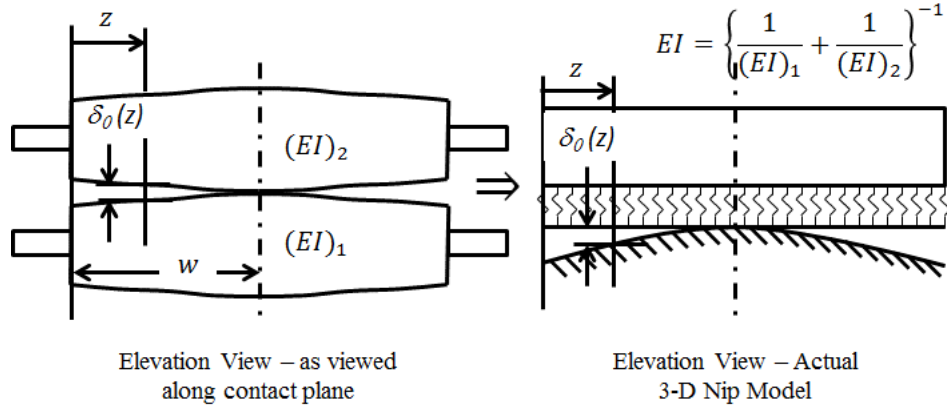Figure 5 – Load/Engagement Functional Relationship, General Situation

Figure 6 – General Diameter Input Scheme

Roller Axes Skew and Crowning

Roller axes skew and crowning can be added to the model in terms of a properly defined axial distribution of radius non-uniformity. Referring to Figure 7, we determine this dependence as follows. First, from Figure 7, we define roller axes skew, ϕ, in terms of an end misalignment, x_e, with the pivot location midway across the roller face:

$$\phi = roller\ skew = \frac{x_e}{w} \qquad \{20\}$$

Application of the Pythagorean theorem at the end of the roller (section a-a, Figure 7) yields the following relationship between the variables:

$$\left(r_s + \delta_{0,skew}(z=0)\right)^2 = x_e^2 + r_s^2 \qquad \{21\}$$

This expression can be simplified if the last term in the left-hand side is neglected by assuming it to be 2nd order:

$$\delta_{0,skew}(z=0) \approx \frac{1}{2}\frac{x_e^2}{r_s} \qquad \{22\}$$

The general expression for the radius non-uniformity is of the same form as {22} and can be written by recognizing that the offset at arbitrary axial positions is a linear function of axial position:

$$\delta_{0,skew}(z) \approx \frac{1}{2}\frac{\{(w-z)\phi\}^2}{r_s} \qquad \{23\}$$

From {23}, it is seen that skewing the roller axes is equivalent to imposing a parabolic radial profile to the roller. Using a similar analysis and again neglecting higher order terms, it can easily be shown that a crowned roller (with a radius difference center-to-end, Δr_s) will have the parabolic dependency on axial position:

$$\delta_{0,crown}(z) \approx \frac{(w-z)^2 \Delta r_s}{w^2} \qquad \{24\}$$

10

and consequently, that by equating {23} and {24} that roller skew and roller crowning are equivalent means to compensate for shell deflection:

$$\Delta r_s = \frac{1}{2}\frac{w^2\phi^2}{r_s}, crowning\ to\ compensate\ for\ skewing \qquad \{25\}$$

$$\phi = \frac{\sqrt{2r_s\Delta r_s}}{w}, skewing\ to\ compensate\ for\ crowning$$

Before leaving this section, it is of interest to develop a relationship for either skewing or crowning that enables compensation for a non-uniform end-to-center footprint in an end loaded nip roller system that is otherwise aligned and cylindrical. If the footprint is assumed to be a purely geometric function of rubber engagement, it can easily be shown that the engagement difference can be expressed by the following:

$$\Delta\delta_{bend} = \frac{1}{8}(b_e^2 - b_c^2)\left(\frac{r_1+r_2}{r_1r_2}\right) \qquad \{26\}$$

where b is the footprint length at the end ($z = 0$) and the center ($z = w$) of the nip roller. To compensate using skew, the engagement difference replaces the change in roller radius in the second of {25}:

$$\phi = \frac{\sqrt{2r_s\Delta\delta_{bend}}}{w}, skewing\ to\ compensate\ for\ bending \qquad \{27\}$$

and to compensate using crowning, the engagement difference is directly applied to the nip roller pair.
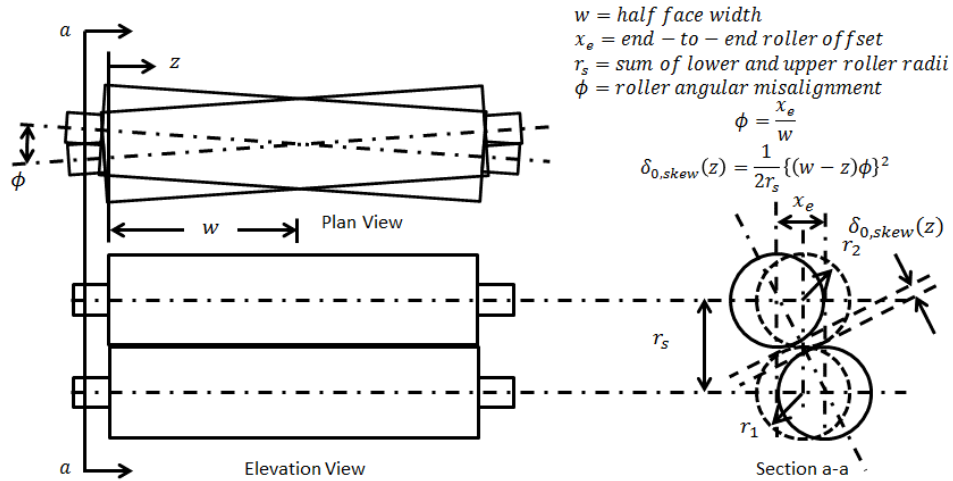

Figure 7 – Roller Skew Axes Input Scheme

RESULTS AND DISCUSSION

The model presented was verified by comparison to experimental results from Good [3]. In that paper, the system of interest is a pair of symmetrically loaded rubber-covered lamination nip rollers. Geometric inputs consist of the following: journal lengths of 6.03

cm, shell lengths of 75.88 cm and shell outer diameters of 80 mm and inner diameters of 54 mm. The rubber coverings are 4 mm thick and have a hardness of 70 IRHD. Nip loading was achieved by pneumatic cylinders at the roll ends. Two loading cases were tested. In the low loading case, an average of 1508 N was applied to the ends and in the high loading case, an average of 2141N was applied to the ends. Results were obtained by examination of Figure 15 from [3]. For comparison to the new model, results across the width were averaged to provide a symmetrical set of results for each loading condition since the new model assumes width-wise symmetry in the boundary conditions. Comparison of results from the new model are shown in Figure 8. Four sets of information are presented: nip load, footprint, creep strain and maximum centerline stress in the nip, all as a function of position along the shell. To achieve these results, it was necessary to first evaluate the 2-D nip behavior using the model from Cole [1]. To achieve the results shown in Figure 8, an elastic modulus of 5.98 MPa and a Poisson's ratio of 0.495 were used. As can be seen, the agreement between measured and predicted nip load is very good and thus, the new model is judged to be quite capable of predicting the various nip responses of interest.
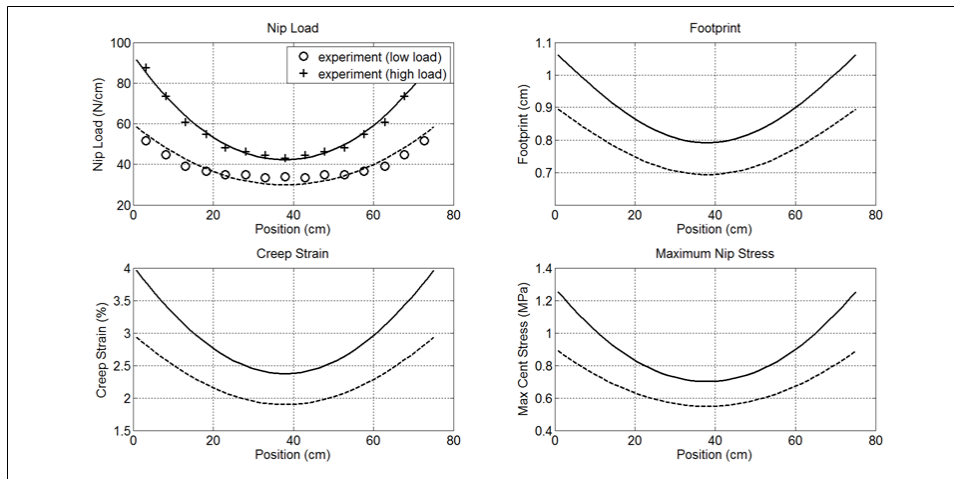

Figure 8 – Comparison of New Model to Good [3]

The new model can now be used to study the effect of roller crowning. Results from such a study are presented in Figure 9. Five sets of data corresponding to five different amounts of crown are shown (0.0000, 0.0625, 0.1270, 0.1819 and 0.1905 mm) where 0.1819 mm corresponds to that computed from {26}. The results are for the "low load" conditions (1508 N average end loading) and are representative of how the system responds. Several things are noted from these results. First, the nip responses indicate significant variation along the axis of the shell with the highest responses at the ends and the lowest responses midway across when crowning is not employed. Second, as crowning increases, the expected behavior is indicated, namely, that the responses tend to become more uniform across the width. Third, the amount of crowning based on the use of {26} appears to overestimate what is required to compensate for shell deflection. This is indeed the case and is a direct consequence of the fact that the rubber covering does not behave per the geometric assumption contained in {26}. The reason is that at higher nip

loadings, less engagement is required to develop a footprint of a particular length due to nearly incompressible behavior of the rubber.
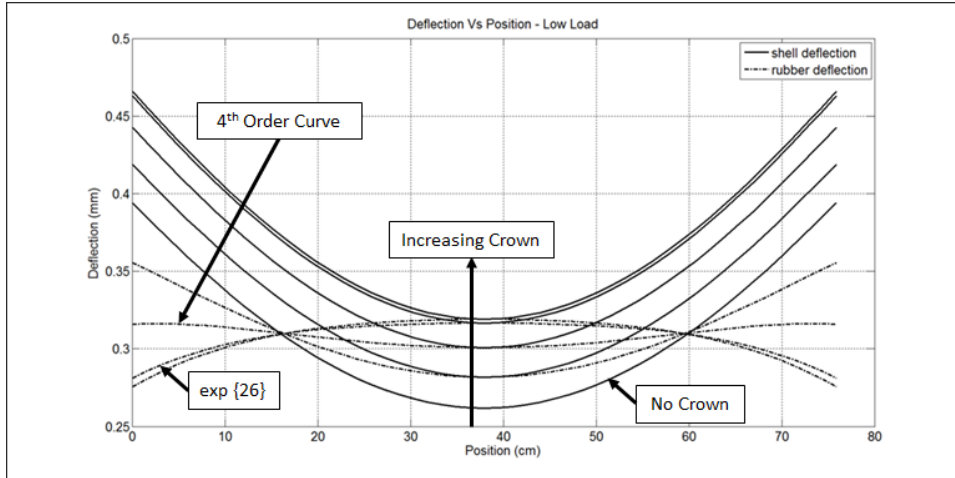

Figure 9 – Model Results, 5 Levels of Crown (low load)

The effect of the incompressible nature of the rubber as a function of loading is shown in Figure 10. Here, we plot end-versus-center nip load difference versus crown as a parametric function of load level. Three load levels are shown: 8.76, 39.7 and 59.1 N/cm. The second and third are the two levels from [3] and the first is an arbitrarily selected lower value. The symbols represent values that were modeled. On each curve, the point corresponding to the value of crown computed from {26} is indicated as well. As can be seen, the difference between the optimum crown (achieved when the end-versus-center nip load difference equals zero) and that computed from {26} decreases as loading decreases. This clearly indicates that the effect of rubber incompressibility decreases with decreasing nip load.
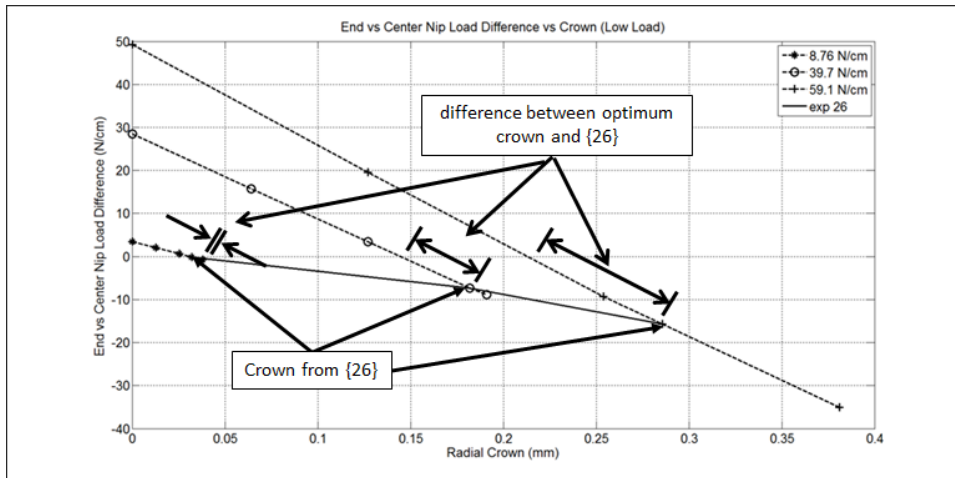

Figure 10 – Model Results, Load Nonuniformity versus Crown

13

More insight can be gained as to the impact of crowning by looking at shell and rubber displacements for the conditions presented in Figure 9. In Figure 11, we plot deflection of the pair of shells and the compression in the rubber for the same five cases of crowning as before. If we define optimum crowning as achieving uniform behavior of the rubber across the width of the shell, then our objective is to pick the level of crown that renders the rubber deflection constant as a function of width. As before, we see that the condition specified by {26} is not that condition and in fact, is too much crown. The third condition, a crown of 0.1270 mm, appears to be closest to achieving this goal. However, it is interesting to note that at best, we will only be able to achieve a profile that achieves a minimum variation, not zero. The reason for this is that we are unable to completely eliminate the effect of shell deflection, which is a fourth order polynomial, by means of a parabolic crown profile. Since crowning is an axial machining process, we can avoid this problem by profiling the appropriate fourth order distribution. However, the same approach cannot be achieved by skewing the roller axes, since skewing creates an inherently parabolic profile and thus, skewing is not as capable a method for achieving nip uniformity.
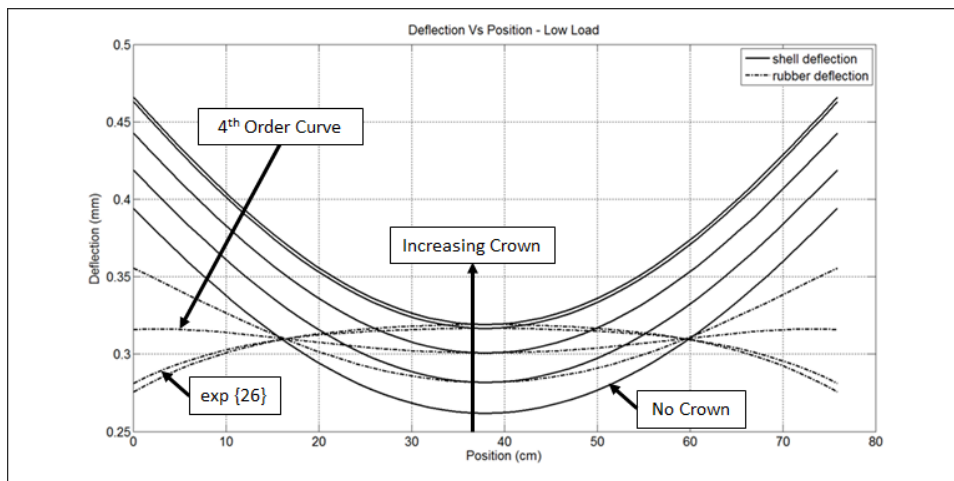

Figure 11 – Model Results, Shell & Rubber Deflection, 5 Levels of Crown (low load)

The results shown so far indicate that it is possible to achieve a fairly uniform nip distribution using either crowning or axes skewing and a completely uniform nip distribution using axially dependent crowning of a higher order distribution. The question might be asked as to whether crowning or skewing is an unfavorable option for other reasons. Figure 12 presents the answer to one consideration regarding crowning. When nips are axially nonuniform due to shell deflection, there will be a symmetrical speed difference across the width due to nip mechanics. This variation will be eliminated when the appropriate amount of roller crowning is used. However, when crowning is used to eliminate shell deflection, there will instead be a symmetrical speed difference due to diameter differences. A comparison of these two speeds are shown in Figure 12. As can be seen, the speed difference due to crowning is less than half of that due to bending. Thus, at first glance, crowning appears to offer a benefit in terms of reducing width-wise speed differences while simultaneously improving nip uniformity. Whether this is the case will depend in large degree to which type of speed difference is more detrimental to

web handling as that due to bending tends to be a web spreading action (edges move faster than center) while that due to crowning tends to be a web gathering action (center moves faster than edges). Skewing, on the other hand, would seem to be problematic from the standpoint of roller alignment and consequently, the heightened risk of shear-induced troughing and wrinkling.
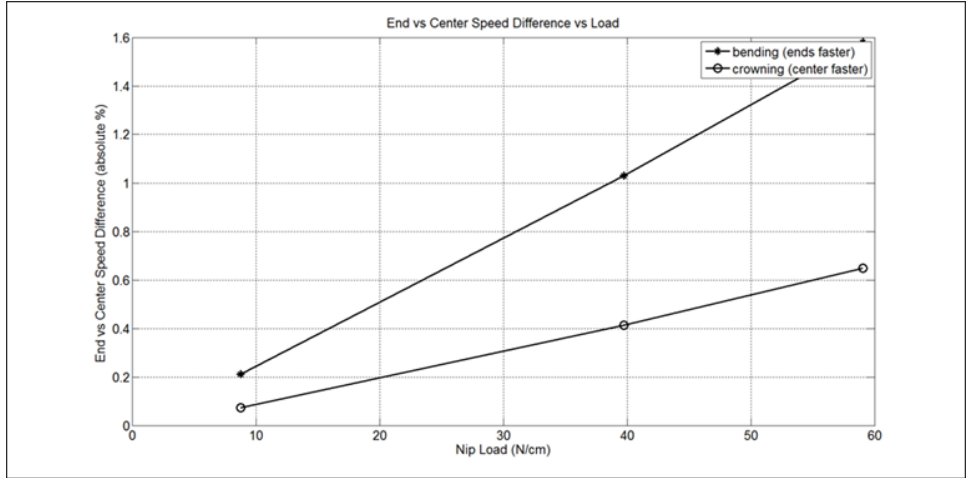

Figure 12 – Model Results, Speed Differences versus Crowning (using {26} values)

SUMMARY

End loaded rubber covered nip roller systems exhibit axial variability due to the combined effects of shell bending and rubber compressibility. The behavior of these systems is non-linear due to the two-dimensional compressible nature of the rubber coverings used in these systems. A three-dimensional model has been presented that accounts for these combined effects and is based on the concept of transfer matrices, which utilize incremental linear shell deflection solutions to capture the impact of the non-linear rubber compressibility behavior. An extension to the model which enables the inclusion of gapping both before and during loading has also been presented. It has also been shown how this capability can be used to study the impact of roller radial crowning and axes skewing. It is further explained how these techniques can be used to compensate for roller shell deflection to achieve a more uniform axial nip profile. The model has been verified by comparison to experimental data [3].

Relationships have been presented that demonstrate the appropriate relationship between crowning and axes skewing to achieve an equivalent reduction in nip axial non-uniformity due to shell bending. Additionally, a relationship indicating crown magnitude based on footprint edge-to-center difference for a cylindrical, aligned nip roller system is also presented. It is demonstrated that for conventional rubber covered systems, where the rubber is very nearly incompressible, that this expression tends to overpredict the amount of crowning required to compensate for shell bending. The magnitude of the error tends to be higher as loading is increased and is essentially a consequence of the characteristic of rubber to exhibit positive circumferential strain as radial loading is increased. It is further shown that crowning may be preferred over skewing since the axial speed difference due to crowning, for the case studied in this paper, is much less than that due to creep from bending and furthermore, does not lead to angular tracking

15

such as would be possible with skewing. A further benefit of crowning is that it can be applied with an axial distribution to completely eliminate the effect of shell bending. This is unlike skewing, which is essentially generates an initial parabolic axial gapped profile.

REFERENCES

1. Roisum, D. R., The Mechanics of Rollers, <u>Tappi Press</u>, 1996, pp. 69-90.
2. Cole, K. A., "Modeling of Nip Pressures and Web Feed Rates in Rubber Covered Nip Rollers," <u>Proceedings of the 12th International Conference on Web Handling</u>, Oklahoma State University, Stillwater, Oklahoma, June 2013.
3. Good, J. K, "Modeling Rubber Covered Nip Rollers in Web Lines," <u>Proceedings of the 6th International Conference on Web Handling</u>, Oklahoma State University, Stillwater, Oklahoma, June 2001, pp. 159-177.